Development 137, 2795-2804 (2010) doi:10.1242/dev.051300

The time to measure positional information: maternal Hunchback is required for the synchrony of the Bicoid transcriptional response at the onset of zygotic transcription

Aude Porcher[1,2], Asmahan Abu-Arish[3,*,†], Sébastien Huart[1,2,†], Baptiste Roelens[1,2,†], Cécile Fradin[3,4] and Nathalie Dostatni[1,2,‡]

SUMMARY

It is widely accepted that morphogenetic gradients determine cell identity by concentration-dependent activation of target genes. How precise is each step in the gene expression process that acts downstream of morphogens, however, remains unclear. The Bicoid morphogen is a transcription factor directly activating its target genes and provides thus a simple system to address this issue in a quantitative manner. Recent studies indicate that the Bicoid gradient is precisely established in *Drosophila* embryos after eight nuclear divisions (cycle 9) and that target protein expression is specified five divisions later (cycle 14), with a precision that corresponds to a relative difference of Bicoid concentration of 10%. To understand how such precision was achieved, we directly analyzed nascent transcripts of the *hunchback* target gene at their site of synthesis. Most anterior nuclei in cycle 11 interphasic embryos exhibit efficient biallelic transcription of *hunchback* and this synchronous expression is specified within a 10% difference of Bicoid concentration. The fast diffusion of Bcd-EGFP (7.7 $\mu m^2/s$) that we captured by fluorescent correlation spectroscopy in the nucleus is consistent with this robust expression at cycle 11. However, given the interruption of transcription during mitosis, it remains too slow to be consistent with precise de novo reading of Bicoid concentration at each interphase, suggesting the existence of a memorization process that recalls this information from earlier cycles. The two anterior maternal morphogens, Bicoid and Hunchback, contribute differently to this early response: whereas Bicoid provides dose-dependent positional information along the axis, maternal Hunchback is required for the synchrony of the response and is therefore likely to be involved in this memorization process.

KEY WORDS: Morphogenetic gradients, Precision of patterning, Transcription, *Drosophila*

INTRODUCTION

Morphogenetic gradients are used by numerous organisms to instruct cell fate as a function of position in a field of cells and establish axial polarities (Ashe and Briscoe, 2006; Ibanes and Belmonte, 2008). In these systems, it is generally accepted that cells are able (1) to measure their position relative to the source of morphogen by detecting its concentration and (2) to turn on accordingly the expression of the various target genes responsible for their identity. Although the crucial role of morphogens in axial patterning is now well established, it remains unclear how precisely the morphogen concentration is detected by the cell and how precise each step in the expression process acting downstream is. The Bicoid (Bcd) morphogen is maternally expressed as an exponential concentration gradient along the anteroposterior (AP) axis of *Drosophila* embryos and is itself a DNA-binding transcription factor that directly activates expression of its target genes in distinct anterior domains (Driever and Nusslein-Volhard, 1988a; Driever and Nusslein-Volhard, 1988b). It therefore provides a simple system with which to analyze the functioning of such gradients in a precise quantitative manner (Porcher and Dostatni, 2010). Recent quantitative measurements of Bcd concentrations, using fluorescently tagged Bcd (Gregor et al., 2007b), have shown that the gradient is already established with high precision in cycle 9 embryos, at the beginning of zygotic transcription (Fig. 1A). In most studies, the Bcd response has been monitored at cycle 14, five nuclear divisions later (Fig. 1A), using enzymatic detection of target transcripts (Bergmann et al., 2007; Crauk and Dostatni, 2005; Lebrecht et al., 2005) or immunofluorescent detection of target proteins (Bergmann et al., 2007; Gregor et al., 2007a; Manu et al., 2009). In contrast to the smooth decrease of Bcd concentrations from anterior to posterior, expression domains of the Bcd target genes display sharp posterior borders at cycle 14. Recent data indicate that, at cycle 14, adjacent nuclei expressing significantly different levels of the Hunchback (Hb) target protein at the border of its expression domain only contain a relative difference of Bcd concentration ($\delta C/C$) of 10% (Gregor et al., 2007a). The minimal period required to reach these accurate responses was estimated by assuming that the limiting step in the process was the random arrival of Bcd molecules to their binding sites (Bialek and Setayeshgar, 2005; Gregor et al., 2007a). According to the slow diffusion coefficient (0.27 $\mu m^2/s$) of Bcd determined by fluorescence recovery after photobleaching (FRAP) in the cortical cytoplasm (Gregor et al., 2007b), this period was estimated to be ~2 hours, a value close to the time period between egg deposition to cycle 14 (Fig. 1A). It was thus proposed that, despite the precise establishment of the Bcd gradient in 1 hour, its primary transcriptional response, which may occur as early as cycle

[1]Institut Curie, Paris, F-75248 France. [2]CNRS, UMR218, Paris, F-75248, France. [3]Department of Physics and Astronomy, McMaster University, Hamilton, Ontario, L8S 4M1, Canada. [4]Department of Biochemistry and Biomedical Sciences, McMaster University, Hamilton, Ontario L8N 3Z5, Canada.

*Present address: Department of Physics, McGill University, Montreal, Quebec, H3A 2T8, Canada
†These authors contributed equally to this work
‡Author for correspondence (nathalie.dostatni@curie.fr)

Accepted 9 June 2010

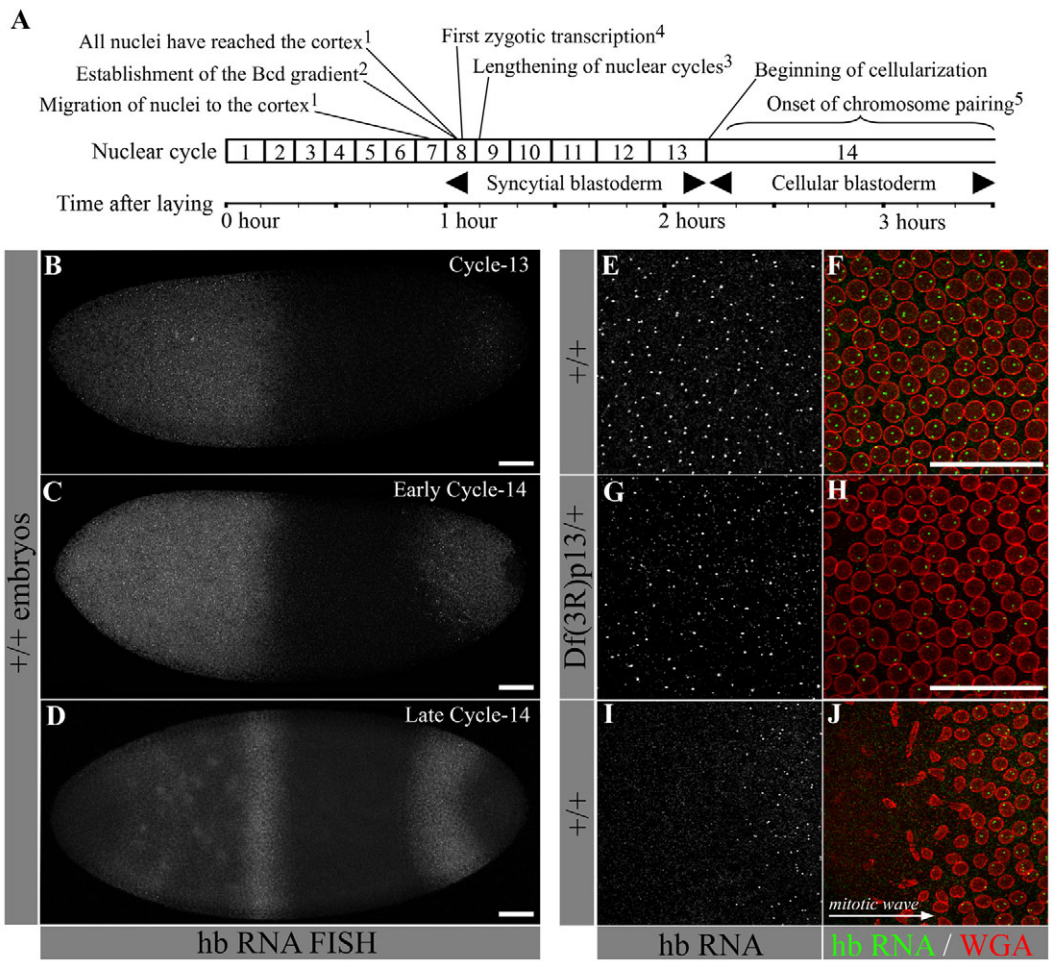

Fig. 1. Nascent transcripts detected by RNA-FISH at the *hb* locus. (**A**) Major events occurring during early *Drosophila* embryogenesis. [1](Foe et al., 1993); [2](Gregor et al., 2007b); [3](Sibon et al., 1997); [4](Pritchard and Schubiger, 1996); [5](Hiraoka et al., 1993). (**B-E**) *hb* transcripts detected by FISH on wild-type embryos at cycle 13 (B), early cycle 14 (C) and late cycle 14 (D). (**F-J**) Magnification of *hb* RNA-FISH in the anterior half of embryos in white (E,G,I) or in green, combined with nuclear membrane detection in red (F,H,J). Embryos were wild type (E,F,I,J) or heterozygous for Df(3R)p13 (G,H). Embryos were in interphase-13 (E-H) or exhibited a mitotic wave during mitosis 12 (I,J). Images projected from 10 (B-D) and 5 (E-J) *z*-stacks. Anterior is leftwards. Scale bars: 50 μm.

8 (Fig. 1A), cannot be precise and that the precision acquired thereafter might involve communications among nearby nuclei (Gregor et al., 2007a). Based on the expression of target proteins in late cycle 14 embryos, a recent model proposes that precision of AP patterning involves downstream cross-regulations among Bcd target genes, which mostly encode transcription factors (Manu et al., 2009).

To gain insights into the process that controls the precision of the Bcd response, we used fluorescent in situ hybridization (RNA-FISH) to directly detect nascent transcripts of the main Bcd target gene [*hunchback* (*hb*)] accumulating at their site of synthesis. This allowed us to distinguish unambiguously the maternal and zygotic expressions of *hb*, which largely overlap in syncytial embryos and so far have been a major hindrance for the analysis of the Bcd response before nuclear cycle 14 (Fig. 1A). In addition, by monitoring transcription at each *hb* locus, RNA-FISH provided access to the earliest possible step in the gene expression process and therefore avoided delay and/or additional mechanistic steps in measuring the Bcd response. Finally, detection of *hb* transcripts at their site of synthesis provided access to the dynamics of transcription at the scale of the *hb* loci and quantified the probability for an *hb* locus to be in an active or inactive transcriptional state. This approach indicated that *hb* transcription reaches a precise and synchronous optimum in cycle 11 interphasic embryos soon after the beginning of zygotic transcription and the steady establishment of the gradient. At the level of the whole embryo, the *hb* transcription domain is positioned along the AP axis with a precision corresponding to 2-3% of egg length (EL), similar to the precision observed for the Bcd fluorescent gradient itself [see Fig. 5C in Gregor et al. (Gregor et al., 2007a)]. At the molecular level, *hb* transcription is specified within a relative difference of Bcd concentration of 10%. Measurements of the mobility of Bcd in syncytial nuclei using fluorescent correlation spectroscopy (FCS) returned a diffusion coefficient of 7.7 $\mu m^2/s$ for a large fraction of the Bcd molecules. This is compatible with the synchrony and precision of the response at cycle 11. Finally, genetics indicate that, whereas Bcd provides dose-dependent positional information along the axis, maternal Hb contributes to the synchrony of the response at cycle 11 and provides temporal information to the system in a dose-dependent manner.

MATERIALS AND METHODS

Fly stocks

Fly stocks include the *bcd[6]* (*bcd*^{E1}) and *hb[15]* (*hb*^{FB}) alleles, *Df(3R)p13* deficiency (# 1943, Bloomington), transgenes expressing Bcd-EGFP (Gregor et al., 2007b) or NLS-EGFP (Gregor et al., 2008) gradients, a transgene expressing H2AvDGFP fusion (Clarkson and Saint, 2004), and the *TM3 (P[w[+mW.hs]=Thb8-lacZ]WD1, Sb[1] Ser[1]*) balancer (# 4860, Bloomington).

RNA-FISH

hb and *lacZ* probes were complementary to their entire mRNA and were prepared using digoxigenin or biotin labeling mixes (Roche). Hybridization were performed as described previously (Bellaiche et al., 1996). For

fluorescent staining, hybridized embryos were washed for 3×15 minutes, incubated for 2 hours with a 1/400 dilution of a mouse anti-digoxigenin antibody (Roche), washed for 4×20 minutes and incubated 1 hour in a 1/400 dilution of an AlexaFluor-488 anti-mouse antibody (Molecular Probes). After 4×20 minutes washes, embryos were stained in DAPI (5 μg/ml) and a 1/500 dilution of WGA-AlexaFluor-633 (Molecular Probes), and washed for 4×15 minutes before mounting. All washes were in PBT (PBS, 0.1% Tween 20) and all antibody dilutions were in the blocking reagent (Roche).

Microscopy

Embryos were mounted in Vectashield (Vector) and imaged using a Zeiss LSM 510 confocal microscope (40×, 1.3 NA). Three-dimensional acquisitions were performed with 1 μm spaced *z*-stacks and a pinhole set at 1 μm ~1.09 Airy Unit function of the laser. The pixel size was 0.31 μm. The AlexaFluor-488, AlexaFluor-568 and AlexaFluor-633 were excited, respectively, by a 488, 543 or 633 nm laser. For each *z*-stack, three acquisitions were required to image the whole embryo and the multi-time macro from the LSM510 software allowed images stitching. Given the Rabl orientation of chromosomes, all nuclear bright dots were found in seven or eight consecutive *z*-stacks.

Image analysis

To ensure that embryos were comparable in their developmental timing, only interphasic embryos (DAPI staining) harboring nuclei with an average cross-section between 80 and 120 μm^2 (WGA staining) were selected for analysis and segmented in two dimensions in one of the median *z*-stacks. Cycle 9 to cycle 12 embryos were mostly segmented automatically using the watershed plug-in (ImageJ), whereas hand processing was required for cycle 13 embryos. For 3D analysis and nuclear volume detection, each nucleus was extrapolated to be a tubular structure with, in each *z*-stack, the section identified by the segmentation in two dimensions. A minimal detection threshold of bright dots (≥3 voxels) was defined for each embryo and applied to all individual nuclei. It was fixed to the lower limit avoiding the detection of aberrant nuclei with more than two bright dots. To verify that most bright dots were detected inside nuclei, the 3D Object Counter plug-in (ImageJ) was used to process the whole embryo. The numbers of dots detected with each method were compared for each embryo and the difference was verified to be below 5%.

Statistics and quantification

Densities of *hb*-expressing nuclei as a function of position along the AP axis were obtained from R (A language and environment for statistical computing, http://www.R-project.org). The numbers of nuclei containing one, two, or one or two bright dots were estimated at 500 positions along the AP axis using a Kernel Density Estimation method with a smoothing bandwidth of 2% EL. Distributions, indicated as a percentage of nuclei containing one, two, or one or two *hb*-active loci, were normalized to the overall distribution of nuclei. In the rare cases in which the graph contained two points of local maximal derivative at the border, the position of the border was chosen as an average between these two positions attributing a relative weight to each point depending on its derivative. To distinguish the variability of the shape of the border (output noise) from the variability of the position of the border (input noise), each graph was shifted along the AP axis from the position of its border to the mean position at a given cycle. For each nuclear cycle, an average graph was then calculated using shifted graphs of individual embryos. The slope (S) of the average graph at the point of maximal derivative was used to quantify the width of the border as equal to the mean value of the distribution plateau (in general between 80% and 60% EL) divided by S. The precision of the response at the molecular scale level was then inferred from the calculation of the minimal distance between nuclei (from 30% and 70% EL) exhibiting significantly different probabilities to express *hb*, using the Fisher's exact test, on the shifted distributions for the *n* embryos analyzed at each cycle. The statistical test used to evaluate the significance of variation in biallelic expression of *hb* was the Mann-Whitney-Wilcoxon test with the Holm correction of the *P* value. It was well adapted to account for the low number of samples.

Fluorescence correlation spectroscopy

Measurements were performed using a home-built instrument (Banks and Fradin, 2005) in exactly the same way and using the same instrument settings as for the cytoplasmic measurements that have already been described in details elsewhere (Abu-Arish et al., 2010). Exceptionally, individual measurements were excluded from the data sets if the fluorescence intensity was not constant over the course of the experimental run (less than 5% of all measurements). Data were analyzed under the assumption that two populations of molecules are present with equal specific brightness but different diffusion coefficients (Dittrich et al., 2005). Analysis also took into account the blinking of the EGFP fluorophore (Haupts et al., 1998). Fitting was performed first on individual auto-correlation functions with the blinking parameters allowed to vary (see Fig. S5 in the supplementary material, non-weighted least-square fits), then on the average autocorrelation functions with the EGFP blinking relaxation time fixed at 300 μs (Fig. 5, weighted least-square fits), in both cases using Kaleidagraph (Synergy software).

RESULTS

The *hb* transcription border is already qualitatively sharp at cycle 11

The primary read out of the Bcd response was assessed using RNA-FISH for the main Bcd target gene [*hunchback* (*hb*)] on blastoderm embryos. At the level of the whole embryo, *hb* RNA-FISH profiles (Fig. 1B-D) were similar to those obtained by enzymatic detection (Crauk and Dostatni, 2005). Magnifications of the staining revealed two types of signals: intense bright dots and a more homogenous staining (Fig. 1E). The combination of RNA-FISH with nuclear membrane detection indicated that the bright dots were exclusively nuclear and that no more than two were present per nucleus (Fig. 1F). As previously proposed (Kosman et al., 2004; Shermoen and O'Farrell, 1991; Wilkie et al., 1999), these bright dots likely correspond to nascent transcripts accumulating at their site of synthesis. Accordingly, RNA-FISH staining of embryos that were heterozygous for a large deletion removing the *hb* locus revealed anterior nuclei with no more than a unique bright dot (Fig. 1G,H). In agreement with a global transcriptional repression during mitosis (Gottesfeld and Forbes, 1997; Shermoen and O'Farrell, 1991), these *hb* bright dots were not observed in mitotic embryos (not shown) nor in the mitotic wave (Foe and Alberts, 1983) captured in occasional embryos (Fig. 1I,J). Zygotic transcription at the *hb* loci was first detected in cycle 9 embryos (see Fig. S1 in the supplementary material). It became readily detected at cycle 11 (Fig. 2A,B) and was consistently observed in anterior interphasic nuclei from cycle 12 to cycle 14 (Fig. 2C-H). The domain containing the *hb*-expressing nuclei was limited by a posterior border that was almost linear at cycle 11 and became increasingly convoluted as the number of nuclei increases (Fig. 2A,C,E,G).

Synchronous transcription of the *hb* loci in the anterior of cycle 11 embryos

Image processing enabled the quantitative analysis of RNA-FISH signals. First, the overall fluorescent intensities of bright dots varied from 0.2 to 3 (arbitrary units) for a single embryo. They did not correlate with position along the AP axis (see Fig. S2A-E in the supplementary material) and were therefore largely independent of Bcd concentration. Second, *hb* transcription appeared somewhat dynamic from cycle 9 to cycle 14. At cycle 9 and cycle 10, *hb* transcription was detected in anterior nuclei expressing one or two *hb* loci intermingled with silent nuclei (Fig. 3A,B,F,G). At cycle 11 and cycle 12, most nuclei in the whole anterior half of the embryos express *hb* with (1) the majority of anterior nuclei expressing both

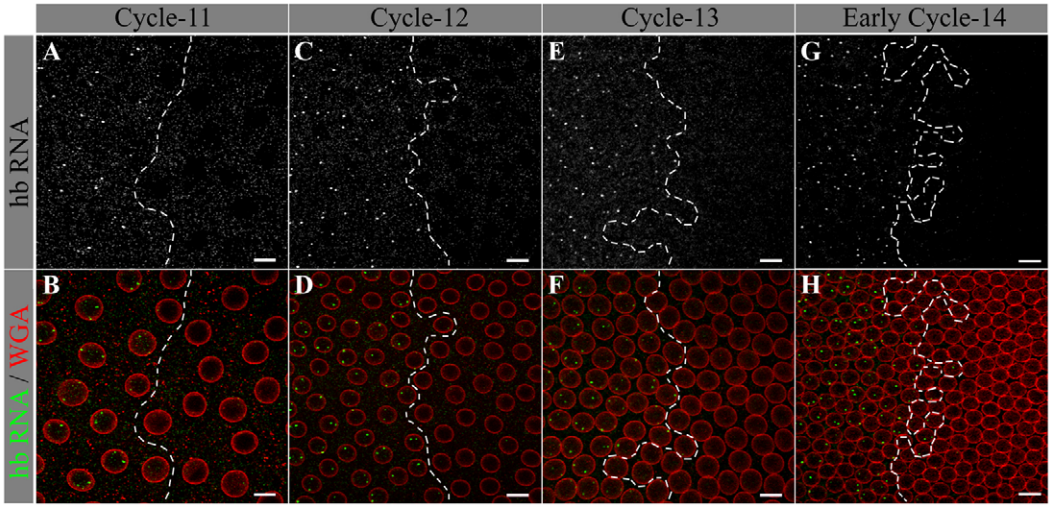

Fig. 2. Expression of the *hb* locus in the middle of the AP axis of syncytial embryos. *hb* RNA-FISH on wild-type *Drosophila* embryos at the border of the expression domain in white (**A**,**C**,**E**,**G**) and in green combined with nuclear membrane detection in red (**B**,**D**,**F**,**H**). Nuclear cycles are indicated at the top. The broken lines delineate the domains with mostly *hb*-active nuclei (left) or *hb*-silent nuclei (right). Images projected from five *z*-stacks. Anterior is leftwards. Scale bars: 10 μm.

hb loci (Fig. 3C,D,H,I) and (2) nuclei expressing a single *hb* locus scattered along the anterior half (Fig. 3C,D) with a slight enrichment at the anterior tip and at the posterior border (Fig. 3H,I, arrowheads). At cycle 13, nuclei expressing both *hb* loci were less abundant and the proportions of anterior nuclei silent for *hb* or exhibiting monoallelic expression of *hb* were higher (Fig. 3E,J). Importantly, given the interruption of transcription during mitosis and the short interphase (6 minutes), the highly synchronous expression detected at cycle 11 and cycle 12 must involve either a very fast novel reading of Bcd concentration at the beginning of each interphase and/or a mechanism to memorize this information from one cycle to the next.

Dynamics and precision of the *hb* transcription border along the axis

Quantitative information concerning the borders of the *hb* expression domains was extracted from the graphs plotting the percentage of nuclei expressing one or two *hb* loci along the axis (Fig. 3F-J and see Fig. S3 and S4 in the supplementary material). In most cases, a unique point of maximal derivative was found in the area of the transcription border and was used, for each embryo, to define the position of this border along the AP axis. The mean position of the border (calculated from four or five embryos at each cycle) appeared somewhat dynamic along the AP axis from cycle 9 to cycle 13 (Fig. 4A): it was found anterior at cycle 9 (~66.2% EL), more posterior at cycle 11 (~50.3% EL) and shifted back towards the anterior at cycle 13 (~57.8% EL). At a given cycle, standard deviation of these positions among embryos was in the range 2-3% EL (Fig. 4A), except at cycle 9 and at cycle 10 for which it was larger, probably as a consequence of the limited number of nuclei (see Fig. S4A,B in the supplementary material). Importantly, this precision of 2-3% EL among embryos is consistent with the precision of the Bcd fluorescent gradient [see Fig. 5C in Gregor et al. (Gregor et al., 2007a)]. Altogether, these RNA-FISH data indicate that, considering the probability of an *hb* locus being activated and the size of the *hb* expression domain, early anterior transcription of *hb* has reached its optimum and is already very robust at cycle 11.

Precision of the response to Bcd at the molecular level

As observed qualitatively (Fig. 2), anterior domains containing *hb*-active nuclei (one or two dots) harbor posterior borders that become more convoluted as the number of nuclei increases. Measurements from the graphs plotting the average transcriptional status of nuclei along the axis (Fig. 4B) indicate that the widths of these borders are of similar magnitude (~8% EL) at all cycles (Fig. 4C). To gain insights into the precision of the Bcd response at the molecular level, we estimated the minimal distance, within the 8% EL-wide border, between two nuclei exhibiting a significantly different probability of expressing *hb* (with $P<0.001$). This precision of the response at the molecular level was 6.4% EL at cycle 9, 4.4% EL at cycle 10 and around 2% EL from cycle 11 to cycle 13 (Fig. 4D). Altogether, these observations indicate that *hb* transcription is already specified at cycle 11 within 2% EL, which corresponds to a relative difference in Bcd concentration (δC/C) of 10%. Importantly, this precision of the transcriptional response at the molecular level is not becoming higher from cycle 11 to cycle 13.

The physical limits for a precise and synchronous response at cycle 11

The RNA-FISH data indicate that *hb* transcription is already precise two nuclear divisions after the steady establishment of the Bcd gradient and the beginning of zygotic transcription. This raises the question of understanding how such a precision is achieved so rapidly given that the minimal period required for the system to measure accurately a relative difference of Bcd concentration (δC/C) of 10% in adjacent nuclei was proposed to be 2 hours (Gregor et al., 2007a). This value was estimated assuming that the limiting step in the process was the random arrival of the Bcd molecules to their DNA-binding sites inside the nucleus. Its calculation was based on the equation $\delta C/C \sim (DacT)^{-1/2}$ (Berg and Purcell, 1977; Bialek and Setayeshgar, 2005) where c is the concentration of Bcd in the nucleus at the *hb* expression border (~4.8 molecules/μm^3), a is the size of the 10 bp Bcd DNA-binding site (~3 nm) and D is the diffusion constant of Bcd in the nucleus. The value of D (1 μm^2/s) used for this calculation (Gregor et al., 2007a) was in the range of the value

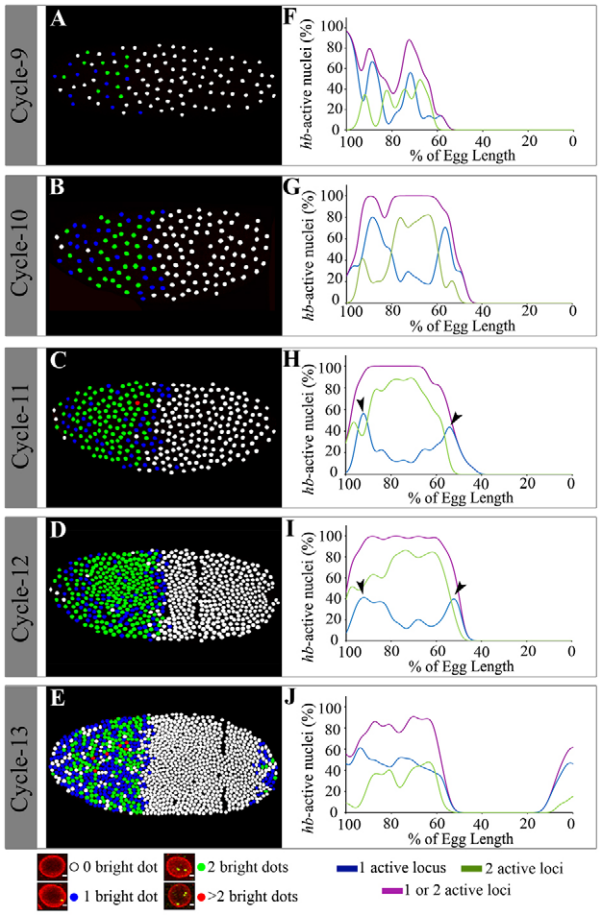

Fig. 3. Highly efficient biallelic expression of *hb* in the anterior half of syncytial embryos. (**A-E**) Simplified fate map of wild-type *Drosophila* embryos after 3D image analysis allows rapid visualization of the *hb* transcription status of each nucleus. The color attributed to each nucleus depends on the number of bright dots that it contained (see legend). (**F-J**) Percentage of nuclei expressing one (blue), two (green), or one or two (purple) *hb* loci indicated for each of the embryo shown in A to E as a function of position along the AP axis. Nuclear cycles are indicated on the left. Anterior is leftwards and positioned at 100% EL.

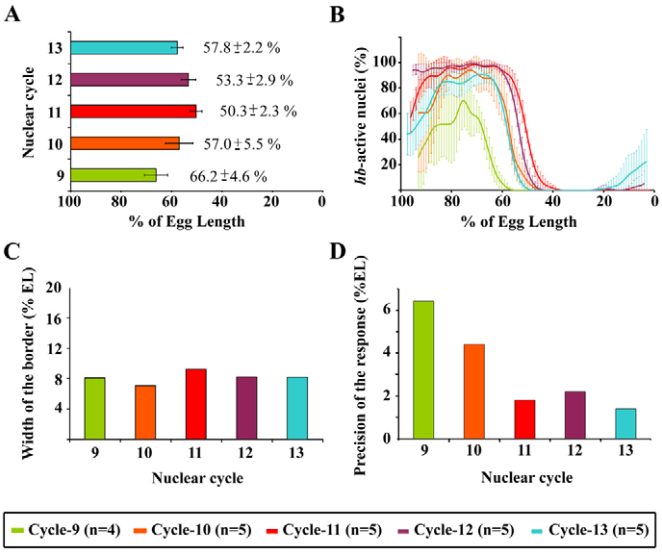

Fig. 4. Position, precision and width of the *hb* transcriptional border from cycle 9 to cycle 13. (**A**) Mean position and standard deviation of the *hb* transcriptional borders, from four or five *Drosophila* embryos at each cycle (raw data are in Fig. S3A-E in the supplementary material). (**B**) Average graphs obtained from individual shifted graphs (see Fig. S3F-J in the supplementary material). Standard deviations to the mean for *n* embryos at each cycle are indicated for one-fifth of the positions regularly distributed along the axis. (**C**) Width of the border at each cycle. (**D**) Precision of the response at the molecular level measured as the minimal distance in the vicinity of the border between two nuclei exhibiting significantly different probability of expressing *hb* with a *P* value of 0.001 (Fisher test). Schematic shows color code for nuclear cycles and number of embryos analyzed.

measured by FRAP (D ~ 0.37 μm^2/s) in the cortical cytoplasm (Gregor et al., 2007b). As it did not correspond to the mobility of Bcd in the nucleus, we decided to directly measure this biophysical parameter of Bcd. For this, instead of FRAP, we used fluorescence correlation spectroscopy (FCS) more adapted to capture the mobility of fast-moving molecules (Sprague and McNally, 2005). Measurements were performed on embryos expressing Bcd-EGFP (Gregor et al., 2007b) or NLS-EGFP (Gregor et al., 2008) gradients. Among the 255 autocorrelation functions (ACF) obtained in anterior nuclei of eight different Bcd-EGFP embryos, all exhibited at least two characteristic decay times, corresponding to at least two different types of motions (see Fig. S5 in the supplementary material). Analysis of the corresponding ACF average was therefore carried out assuming two separate diffusion processes (Fig. 5). The contributions of these two processes split almost evenly, with 57% of the molecules diffusing in the nucleoplasm at 7.7 μm^2/s and the other 43% moving with an apparent diffusion coefficient of 0.22 μm^2/s (Fig. 5C). By comparison, FCS measurements of NLS-EGFP in anterior nuclei showed mobility very close to free diffusion, with 96% of molecules undergoing fast diffusion (28 μm^2/s) (Fig. 5C). Evaluations of Bcd-EGFP concentration in the nucleus from the FCS data [~140 nM at the anterior pole (see Abu-Arish et al., 2010)] were in general agreement with the measurements performed by Gregor and collaborators (Gregor et al., 2007b). The two types of Bcd-EGFP molecules with different mobility detected by FCS in the nucleus allows re-evaluating the minimal period required for the system to achieve a precision of 10%. For this, we used the total concentration of Bcd at the *hb* border (~4.8 molecules/μm^3) and the mean diffusion coefficient considering the relative proportions of each component (7.7×0.57 + 0.22×0.43 ~ 4.5 μm^2/s). Importantly, this allows lowering down this period to ~25 minutes instead of 2 hours. This new value reconciles the rapid development timing of the embryo with the promptness of the precise response to the gradient observed at cycle 11. However, given the short interphase of cycle 11, it remains too large to explain how synchronous transcription at the *hb* loci could be achieved during this interphase from de novo reading of Bcd concentrations. This suggests that the process allowing synchronous expression of *hb* at cycle 11 requires a memorization mechanism allowing each *hb* locus to keep track of the expression status of its parental locus at earlier cycles.

Clonally related nuclei remain grouped in small domains with variable shapes

The RNA-FISH reveal that the *hb* transcription border becomes more convoluted as the number of nuclei increases in the embryos (Fig. 2). This heterogeneity at the border could directly reflect slightly different levels of absolute concentration of Bcd in

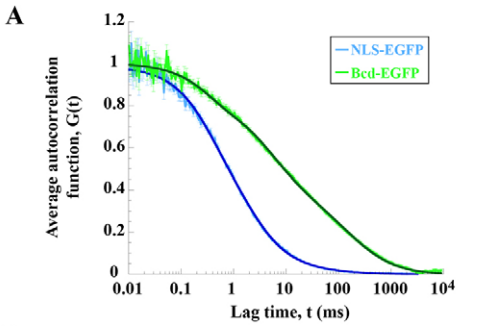

C

	F (%)	D (μm²/s)	F (%)	D (μm²/s)	χ²/υ	n
Bcd-EGFP	57 ± 1	7.7 ± 0.3	43 ± 1	0.22 ± 0.01	0.8	255
NLS-EGFP	96 ± 1	28 ± 1	4 ± 1	0.51 ± 0.04	1	113
	Fast component		Slow component			

Fig. 5. Mobility of the Bcd-EGFP molecules in the *Drosophila* syncytial nuclei. (**A**) Average auto-correlation functions from FCS measurements in anterior nuclei during cycle 13 and cycle 14 for Bcd-EGFP (light green curve) and NLS-EGFP (light blue curve). Dark-green and dark-blue curves indicate fits of the data assuming two independent diffusing species. (**B**) The corresponding residuals are shown for Bcd-EGFP (green) and NLS-EGFP (blue). Residuals have been normalized by the standard error. (**C**) Summary of the parameters identified for the fast and the slow components. F (%) indicates the fraction of a given component and D (μm²/s) its diffusion coefficient. χ^2/υ is the normalized chi-square calculated as described elsewhere (Abu-Arish et al., 2010). *n* is the number of FCS measurements used to calculate the average ACFs shown.

individual nuclei. Alternatively, it could be related to the memorization process, allowing each locus to keep track of its transcriptional history and reflect the shape of the territories of clonally related nuclei in syncytial embryos. To challenge this hypothesis, we performed time-lapse imaging of an embryo expressing a fluorescently tagged H2Av histone and determined at cycle 14, the shape of the territories of clonally related nuclei emerging from specific nuclei identified at cycle 11 (Fig. 6A). This analysis indicated that nuclei emerging from the same parental nucleus at cycle 11 stay together in territories with different shapes and often intercalating (Fig. 6B,C). Importantly, clonally related nuclei are not largely dispersed away from each other during mitosis nor distributed according to regular patterns. The average width of these territories is ~4% EL (Fig. 6D-E). These observations leave open the possibility that the memorization process allowing each *hb* locus to keep track of its transcriptional history from cycle 11 to cycle 14 contributes to the convoluted shape of the *hb* border at cycle 14.

Hb contributes to the synchrony of the response to Bcd at cycle 11

The Hb zinc-finger transcription factor contributes maternally to anterior patterning in synergy with Bcd (Simpson-Brose et al., 1994). To determine Hb contribution in the precision and synchrony of the Bcd response, we analyzed *hb* expression in hb^{FB} heterozygous mutants, which produce hb^{FB} transcripts but a non functional Hb^{FB} protein (Hulskamp et al., 1994). All embryos from heterozygous females expressed only a single dose of functional maternal Hb (Hb^{Mat}) and were zygotically genotyped using a marked chromosome (see Fig. S6 in the supplementary material). At cycle 11, *hb* expression was indistinguishable in all embryos independently of their zygotic genotype (Fig. 7A,B). However, in these embryos, the proportion of anterior nuclei expressing both *hb* loci was lower than in wild-type embryos (dashed curves in Fig. 7C,D). At cycle 12, all embryos from hb^{FB} heterozygous parents harbored a higher number of nuclei expressing both *hb* loci than at cycle 11 (compare Fig. 7A,B with 7E,F). In embryos that were zygotically wild-type, *hb* biallelic expression was found at almost the same level as in wild-type embryos from wild-type females (Fig. 7G,H). By contrast, in embryos zygotically mutant for *hb*, nuclei with *hb* biallelic expression remained under-represented when compared with wild type (Fig. 7G,H). At cycle 13, *hb* expression was similar in all embryos (compare Fig. 7I-L). Finally, the position of the border and its width were not significantly modified by the reduction of the dose of Hb^{Mat} or the absence of zygotic Hb (Hb^{Zyg}) (see Fig. S8 in the supplementary material). These observations indicate that the reduction of the dose of Hb^{Mat} prevents the Bcd gradient from sustaining synchronous expression of *hb* at cycle 11 and that the absence of Hb^{Zyg} at cycle 12 further amplifies this delay. Interestingly, one dose of Hb^{Mat} is sufficient for full response of

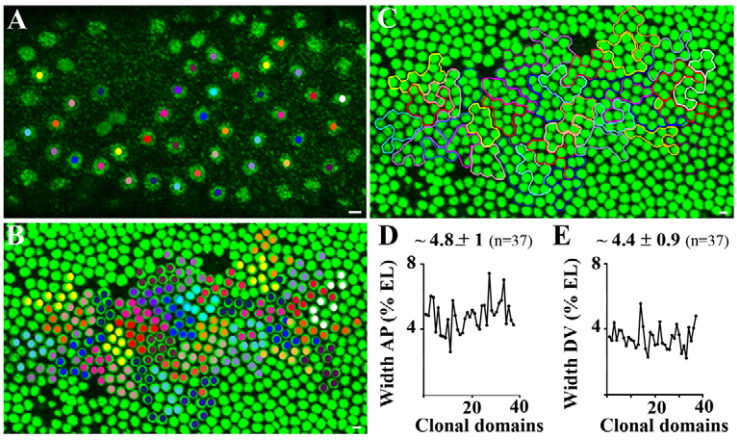

Fig. 6. Shape of territories of clonally related nuclei. (**A**) Confocal view of nuclei in a *Drosophila* embryo expressing the H2Av-GFP at cycle 11. Thirty-seven nuclei were labeled with different colors and followed through three mitotic divisions by time-lapse. (**B**) At cycle 14, the nuclei from the same embryo were labeled with the same color as their parent. (**C**) The borders of the territories of clonally related nuclei (clonal domains) were used to measure the width of each domain along the AP and the DV axis. (**D**) Width of the clonal domains along the AP axis. (**E**) Width of the clonal domains along the DV axis. Scale bars: 5 μm in A-C.

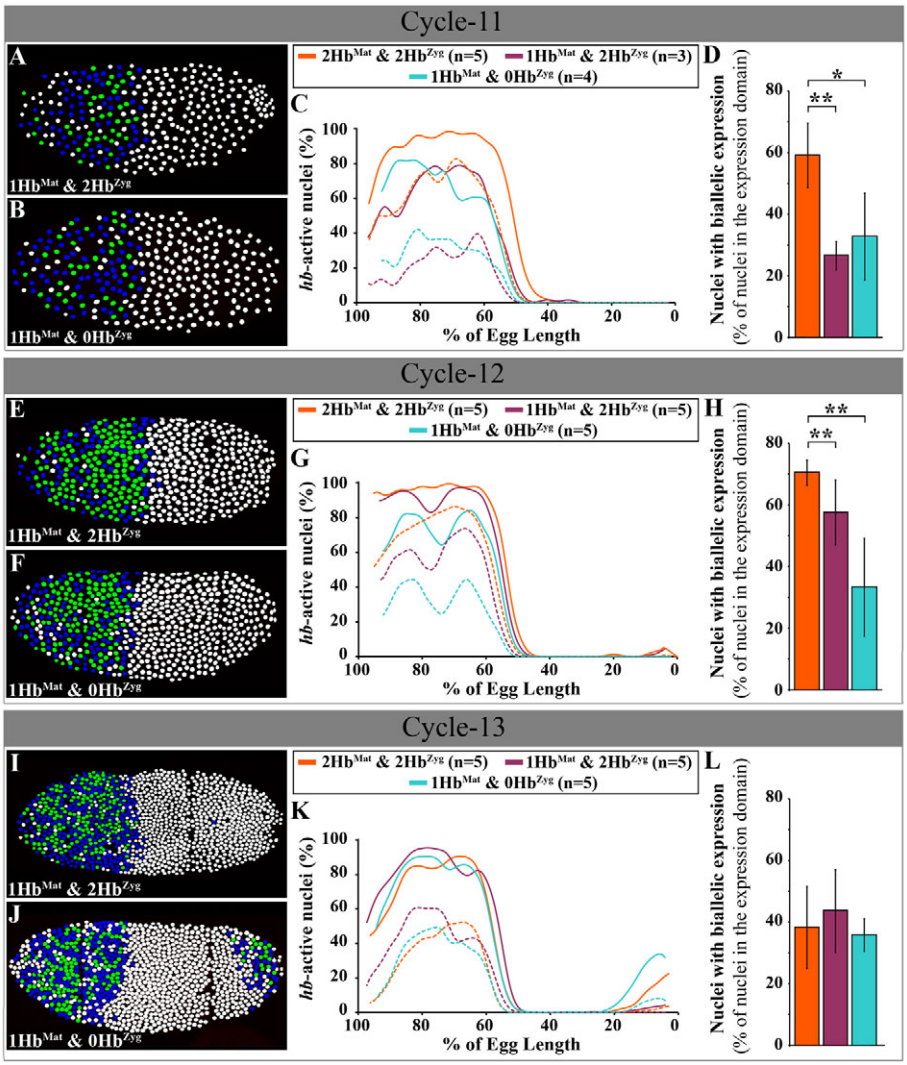

Fig. 7. Maternal and zygotic contributions of Hb to the early Bcd response. *Drosophila* embryos from a cross of hb^{FB}/+ *(Tm3:hb-lacZ)* flies were stained for *hb* and *lacZ* RNA-FISH, zygotically genotyped on the basis of *lacZ* expression (see Fig. S6 in the supplementary material) and processed for quantitative analysis. Embryos from this cross received only a single dose of Hb^{Mat} and were at cycle 11 (A-D), at cycle 12 (E-H) and at cycle 13 (I-L). (**A**,**B**,**E**,**F**,**I**,**J**) Simplified fate map of *hb-lacZ*/*hb-lacZ* wild-type (A,E,I) and hb^{FB}/hb^{FB} mutant (B,F,J) embryos. (**C**,**D**,**G**,**H**,**K**,**L**) Average quantification for several embryos of each genotype (raw data are in Fig. S7 in the supplementary material). (C,G,K) Distributions of nuclei expressing the two (broken lines), or one or two (unbroken lines) *hb* loci. Anterior is leftwards and positioned at 100% EL. (D,H,L) Proportions of nuclei exhibiting biallelic expression of *hb* in the expression domain. Error bars indicate standard deviations. $^{**}P<0.05$; $^{*}P=0.07$ (Mann-Whitney-Wilcoxon test with the Holm correction of the *P* value). Color code for genotype and number of embryos analyzed are indicated for each cycle in the key.

the system at cycle 13 (Fig. 7L). Hb^{Mat} is therefore required for the system to promptly reach a high level of *hb* biallelic expression in anterior nuclei and contributes thus to the early synchrony of the transcriptional response to Bcd at cycle 11. However, Hb^{Mat} does not provide substantial positional information in a dose-dependent manner along the axis.

Bcd is not involved in the early synchrony of the response but provides positional information along the axis

To determine the contribution of Bcd in the kinetics of *hb* expression, we performed RNA-FISH on embryos expressing a single dose of the Bcd gradient. In the expression domain, the overall proportion of nuclei with *hb* biallelic expression was the same in embryos expressing one or two doses of Bcd at cycle 11 (Fig. 8A,C,D) and even earlier at cycle 10 (Fig. 8E,G,H). As expected (Driever and Nusslein-Volhard, 1988a), in embryos from bcd^{E1}/+ females, the *hb* transcription border was shifted towards the anterior when compared with wild type. At cycle 11, a significant shift of ~7% EL was observed (Fig. 8B) but at cycle 10 the variability in the positioning of the border was too high (see Fig. S4 in the supplementary material) to detect a significant shift (Fig. 8F). Finally, the width of the border was identical in embryos expressing one or two doses of Bcd (not shown). Thus, in contrast to Hb, Bcd does not contribute in a dose-dependent manner to the early kinetics of *hb* transcription but provides dose-dependent information for the positioning of the *hb* transcription border the along the axis.

DISCUSSION

Synchronous expression of each hb locus in the anterior of cycle 11 embryos

The efficient biallelic expression of *hb* observed in a majority of anterior nuclei at cycle 11 indicates that this specific response to Bcd reaches a high synchrony much earlier than previously proposed (Gregor et al., 2007a). The absence of transcription during mitosis contrasts with the robust expression during interphase and indicates that transcription is highly dynamic during the rapid nuclear divisions from cycle 9 to cycle 14. Importantly, FCS measurements on the Bcd-EGFP gradients reveal a fast component of Bcd in the nucleus that remains too slow to be consistent with a de novo precise interpretation of its concentration at each interphase. It suggests the existence of a mechanism allowing each locus to keep track of the transcriptional status of its parental locus at earlier cycles. Given the relatively low concentration of Bcd, the short interphase and the diffusion coefficient of the Bcd molecules measured by FCS, a possible scenario is that at the onset of zygotic transcription, the first transcription event at a given *hb* locus would be stochastic with a

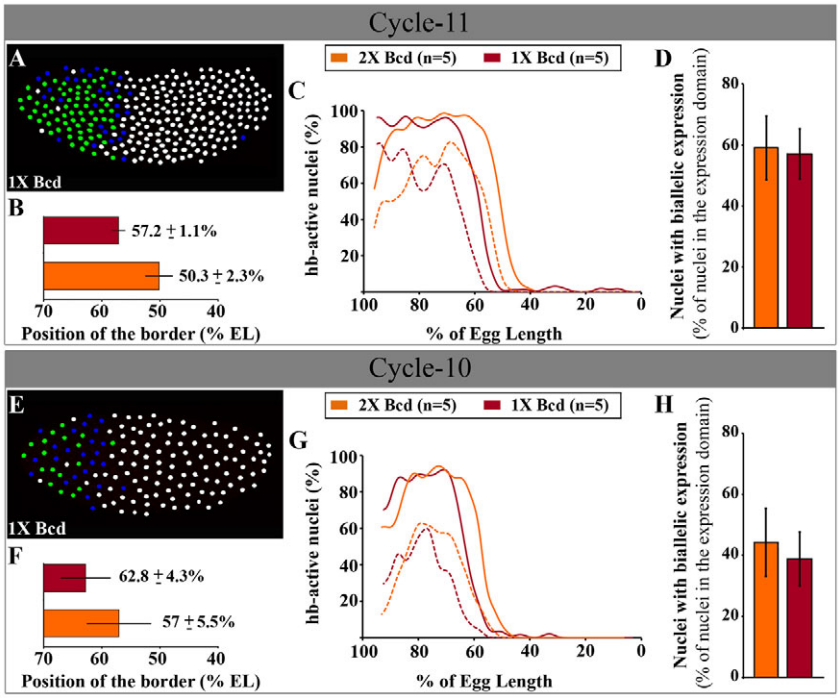

Fig. 8. Dose-dependent contribution of Bcd to the early expression of *hb*. *Drosophila* embryos from bcd^{E1}/+ females were stained for *hb* by RNA-FISH and processed for quantitative analysis. Embryos were at cycle 11 (**A-D**) and at cycle 10 (**E-H**). (A,E) A simplified fate map of a cycle 11 (A) and a cycle 10 (E) embryo. (B-D,F-H) Average quantification for several embryos of each genotype (raw data are in Fig. S9 in the supplementary material). (B,F) Position of the border along the AP axis. (C,G) Average distributions of nuclei expressing the two (broken lines), or one or two (unbroken lines) *hb* loci. Anterior is leftwards and positioned at 100% EL. (D,H) Proportions of nuclei exhibiting biallelic expression of *hb* in the expression domain. Error bars indicate standard deviations. Color code for maternal genotype and number of embryos analyzed are indicated for each cycle in the key.

limited number of loci being activated. After mitosis, each new locus emerging from the replication of an activated locus would maintain activation through a process not strictly dependent on Bcd. By cycle 11, a majority of loci in the anterior would have had a chance to be activated at least once and such a memorization process would allow maintaining expression. The shape of the territories of clonally related nuclei is compatible with the shape of the *hb* transcription border and such a memorization mechanism can also explain why the border is becoming more convoluted as the number of nuclei increases. Time-lapse observation of the Bcd-EGFP gradients did not show colocalization of the Bcd protein with DNA during mitosis (Gregor et al., 2007b) and we did not observe a significant change in *hb* synchrony when reducing Bcd amounts in the embryo. By contrast, *hb* synchrony was reduced at cycle 11 when the dose of maternal Hb was lowered by half. Thus, Hb but not Bcd, is probably involved in this memory mechanism. Such memory process could either involve directly proteins of the transcription machinery maintained on DNA during mitosis such as TFIID (Xing et al., 2008) or chromatin modifications transmitted epigenetically after each division, such as H3K4 methylation (Muramoto et al., 2010). A consequence of such a memory process is that *hb* transcription would be much more dependent on Bcd thresholds at early cycles than at later cycles. This could explain why patterning along the AP axis is highly sensitive at early cycles (cycle 9 and cycle 10) and much less sensitive at later cycles (cycle 11 to cycle 13) to environmental perturbations induced by micro-fluidics devices destroying the Bcd gradient (Lucchetta et al., 2005; Lucchetta et al., 2008).

The fast component of Bcd in the nucleus

The identification of a fast component of Bcd using FCS raises the issue of potential discrepancies between FRAP and FCS measurements of the mobility of Bcd. Importantly, the FRAP measurements performed by Gregor and collaborators in the cytoplasm (Gregor et al., 2007b) cannot be rigorously compared with our FCS measurements in the nucleus. However, we also performed FCS on Bcd-EGFP gradients in the cytoplasm. We found that the Bcd-EGFP molecules in the cytoplasm also had a larger diffusion coefficient than had been observed by FRAP. However, as there are important technical issues when comparing FRAP and FCS (Sprague and McNally, 2005), and as these observations also raise critical issues concerning the establishment of the Bcd gradient in the cytoplasm, they have been the subject of another study (Abu-Arish et al., 2010). Nevertheless, the FCS measurements described in the present study provide the first direct measurements of the mobility of Bcd in the nucleus and this is clearly the critical parameter to evaluate the period required for a precise response inside the nucleus. These measurements reveal the existence of a fast moving component of Bcd that allowed lowering this period to 25 minutes.

The loss of synchrony in *hb* transcription at cycle 13

The biallelic expression of *hb*, at cycle 11 and cycle 12, contrasts with its more heterogeneous transcription at cycle 13 and cycle 14 (see Fig. S10 in the supplementary material). As thresholds used to detect transcript signals by RNA-FISH were similar at each cycle, the heterogeneity in *hb* transcription at cycle 13 is not likely to be due to a failure in the detection of the FISH signals. It is also not likely to be due to more frequent chromosome pairing, because pairing mostly occurs at cycle 14 (Hiraoka et al., 1993) and because increased chromosome pairing would give rise to only an increase in apparent mono-allelic expression but not to the absence of transcription that is also observed in several anterior nuclei at cycle 13. The loss of *hb* synchrony at cycle 13 could be a consequence of the reduction in chromatin plasticity with cell differentiation (Bhattacharya et al., 2009), which might increase the period required for the Bcd protein and the whole transcription machinery to find their DNA targets. Alternatively, transcription in eukaryotic cells has been proposed to occur in pulses (Golding and Cox, 2006) and the bright dots detected by RNA-FISH at the *hb* loci could reflects such pulses. In this case, pulses at the *hb* loci

would be highly synchronous during the short interphase of cycle 11 and would become less synchronous at cycle 13 as the length of interphase increases. Finally, reduced synchrony of *hb* transcription at cycle 13 could also be related to the synchronous versus stochastic patterns of gene activation observed recently in the *Drosophila* embryo for genes involved in dorsoventral (DV) axis formation and correlated to the 'pre-loading' of PolII in promoter regions (Boettiger and Levine, 2009). Although it is surprising that *hb* expression would be first synchronous at cycle 11 and becomes stochastic at cycle 13, a precise analysis of the amount of PolII pre-loaded at the *hb* promoter at cycle 11 versus cycle 13 is required to clarify this issue.

Scaling and dynamics of the *hb* transcription border along the axis

At the level of the whole embryo, the *hb* border is already positioned at cycle 11 with a precision of 2-3% EL, which is remarkably similar to the precision of the Bcd protein gradient itself [see Fig. 5C in Gregor et al. (Gregor et al., 2007a)]. The movement of the position of the *hb* expression border, backwards and forwards to the anterior pole from cycle 9 to cycle 13, indicates that despite the stability of the Bcd gradient along the AP axis (Gregor et al., 2007b), the Bcd thresholds required for *hb* expression are slightly different at each cycle. The early shift of the border towards the posterior is consistent with the 'pre-steady state decoding' model (Bergmann et al., 2007), which proposes that the establishment and interpretation of the gradient occur simultaneously and that feedback mechanisms allow the system to be more robust. However, this early shift occurs after the convergence of the gradient to its steady state (Gregor et al., 2007b) and our analysis indicates that precise and synchronous transcription of *hb* at cycle 11 does not involve feedback autoregulation by Hb^{zyg}. Thus, this early posterior shift of the *hb* expression border is more likely to reflect a progressive establishment of zygotic transcription in replacement of the highly efficient DNA replication process (Pritchard and Schubiger, 1996). Similarly, the shift of the *hb* transcription border towards the anterior from cycle 11 to cycle 13 indicates that the Bcd thresholds required for *hb* expression are slightly higher at cycle 13 than at cycle 11. This latter anterior shift could reflect changes in the transcription process itself owing to reduced chromatin plasticity or accessibility as cell differentiation takes place. It could also indicate that, at cycle 13, the expression of *hb* is no longer under maternal control by Bcd and Hb^{Mat}. Although our experiments exclude the involvement of Hb^{Zyg} in positioning the *hb* transcription border at cycle 13, they do not address the involvement of other sources of AP positional information that act either independently of Bcd, such as information provided by the terminal systems (Löhr et al., 2009; Ochoa-Espinosa et al., 2009), or downstream of Bcd, such as information provided by the other gap proteins Knirps and Krüppel (Manu et al., 2009).

Precision of the Bcd transcriptional response at the molecular level

Detection of *hb* transcripts in nuclei localized at the border allows quantifying the minimal differences of Bcd concentration in nearby nuclei exhibiting different probability to express *hb*. Importantly, this precision of the response at the molecular level is achieved along 2% EL as early as cycle 11 and it is maintained at this level during further nuclear divisions. This precision corresponds to a relative difference of Bcd concentration effectively measured by nearby nuclei ($\delta C/C$) of 10%, and it is similar to the precision observed when analyzing the border of the Hb protein expression domain at cycle 14 (Gregor et al., 2007a). Importantly, our analysis also reveals that the *hb* transcription border becomes more convoluted as the number of nuclei increases in the embryo, indicating that this rule is statistical and not absolute at the level of each individual nucleus. Concerning the precision of the gene expression process acting downstream of transcription, it will be important to determine whether the posterior border of the Hb protein domain is as convoluted at cycle 14 as is the *hb* transcription border or whether an averaging mechanism contributes to straightening this border. Such a mechanism could include the export of the newly transcribed mRNA into the cytoplasm and the random subsequent import of the newly translated nuclear proteins that these mRNA encode into nearby nuclei. Given that the precision of the Bcd transcriptional response is statistically obtained along 2% EL ($\delta C/C$=10%), such a passive averaging mechanism could lead to the expression of the Hb protein in a domain with a rectilinear expression border. Importantly, our data indicate that transcriptional precision does not become higher as the number of nuclei increases in the embryo. Therefore, if more precision is acquired in the expression of the Bcd target proteins during this period (Manu et al., 2009), the process that allows this noise reduction is clearly not controlled at the transcriptional level.

Acknowledgements

We thank Geneviève Almouzni, Edith Heard and Angela Taddei for critical readings of the manuscript; Mathieu Coppey, Paul François, Vincent Hakim, Yuri Okabe, Hervé Rouault and all members of the UMR218 for discussions; Elly Efthymiou and Mathieu Leroux-Coyau for fly care; Eric Wieschaus, Thomas Gregor and the Bloomington stock centre for fly stocks; Patricia Le Baccon, François Waharte and the Imagery platform PICT-IBISA of the Institut Curie. This work was supported by the France-Canada Research Foundation (C.F. and N.D.), the CNRS and the Institut Curie (N.D.), and NSERC (C.F.). C.F. is a recipient of a Canada Research Chair funded by NSERC, A.P. was supported by the University René Diderot and N.D. by INSERM.

Competing interests statement

The authors declare no competing financial interests.

Supplementary material

Supplementary material for this article is available at
http://dev.biologists.org/lookup/suppl/doi:10.1242/dev.051300/-/DC1

References

Abu-Arish, A., Porcher, A., Czerwonka, A., Dostatni, N. and Fradin, C. (2010). Fast mobility of Bicoid captured by fluorescence correlation spectroscopy: Implication for the rapid establishment of its gradient. *Biophys. J.* (in press).

Ashe, H. L. and Briscoe, J. (2006). The interpretation of morphogen gradients. *Development* **133**, 385-394.

Banks, D. S. and Fradin, C. (2005). Anomalous diffusion of proteins due to molecular crowding. *Biophys. J.* **89**, 2960-2971.

Bellaiche, Y., Bandyopadhyay, R., Desplan, C. and Dostatni, N. (1996). Neither the homeodomain nor the activation domain of Bicoid is specifically required for its down-regulation by the Torso receptor tyrosine kinase cascade. *Development* **122**, 3499-3508.

Berg, H. C. and Purcell, E. M. (1977). Physics of chemoreception. *Biophys. J.* **20**, 193-219.

Bergmann, S., Sandler, O., Sberro, H., Shnider, S., Schejter, E., Shilo, B. Z. and Barkai, N. (2007). Pre-steady-state decoding of the Bicoid morphogen gradient. *PLoS Biol.* **5**, e46.

Bhattacharya, D., Talwar, S., Mazumder, A. and Shivashankar, G. V. (2009). Spatio-temporal plasticity in chromatin organization in mouse cell differentiation and during Drosophila embryogenesis. *Biophys. J.* **96**, 3832-3839.

Bialek, W. and Setayeshgar, S. (2005). Physical limits to biochemical signaling. *Proc. Natl. Acad. Sci. USA* **102**, 10040-10045.

Boettiger, A. N. and Levine, M. (2009). Synchronous and stochastic patterns of gene activation in the Drosophila embryo. *Science* **325**, 471-473.

Clarkson, M. and Saint, R. (2004). A His2AvDGFP fusion gene complements a lethal His2AvD mutant allele and provides an in vivo marker for drosophila chromosome behavior. *DNA Cell Biol.* **18**, 457-462.

Crauk, O. and Dostatni, N. (2005). Bicoid determines sharp and precise target gene expression in the Drosophila embryo. *Curr. Biol.* **15**, 1888-1898.
Dittrich, P., Malvezzi-Campeggi, F., Jahnz, M. and Schwille, P. (2005). Accessing molecular dynamics in cells by fluorescence correlation spectroscopy. *Biol. Chem.* **382**, 491-494.
Driever, W. and Nusslein-Volhard, C. (1988a). The bicoid protein determines position in the Drosophila embryo in a concentration-dependent manner. *Cell* **54**, 95-104.
Driever, W. and Nusslein-Volhard, C. (1988b). A gradient of bicoid protein in Drosophila embryos. *Cell* **54**, 83-93.
Foe, V. E. and Alberts, B. M. (1983). Studies of nuclear and cytoplasmic behaviour during the five mitotic cycles that precede gastrulation in Drosophila embryogenesis. *J. Cell Sci.* **61**, 31-70.
Foe, V. E., Odell, G. M. and Edgar, B. A. (1993). Mitosis and morphogenesis in the drosophila embryo: point and counterpoint. In *The Development of Drosophila melanogaster*, Vol. 1 (ed. M. Bate and A. M. Arias), pp. 149-300. Cold Spring Harbor, NY: CSHL Press.
Golding, I. and Cox, E. C. (2006). Eukaryotic transcription: what does it mean for a gene to be on? *Curr. Biol.* **16**, R371-R373.
Gottesfeld, J. M. and Forbes, D. J. (1997). Mitotic repression of the transcriptional machinery. *Trends Biochem. Sci.* **22**, 197-202.
Gregor, T., Tank, D. W., Wieschaus, E. F. and Bialek, W. (2007a). Probing the limits to positional information. *Cell* **130**, 153-164.
Gregor, T., Wieschaus, E. F., McGregor, A. P., Bialek, W. and Tank, D. W. (2007b). Stability and nuclear dynamics of the bicoid morphogen gradient. *Cell* **130**, 141-152.
Gregor, T., McGregor, A. P. and Wieschaus, E. F. (2008). Shape and function of the Bicoid morphogen gradient in dipteran species with different sized embryos. *Dev. Biol.* **316**, 350-358.
Haupts, U., Maiti, S., Schwille, P. and Webb, W. W. (1998). Dynamics of fluorescence fluctuations in green fluorescent protein observed by fluorescence correlation spectroscopy. *Proc. Natl. Acad. Sci. USA* **95**, 13573-13578.
Hiraoka, Y., Dernburg, A. F., Parmelee, S. J., Rykowski, M. C., Agard, D. A. and Sedat, J. W. (1993). The onset of homologous chromosome pairing during Drosophila melanogaster embryogenesis. *J. Cell Biol.* **120**, 591-600.
Hulskamp, M., Lukowitz, W., Beermann, A., Glaser, G. and Tautz, D. (1994). Differential regulation of target genes by different alleles of the segmentation gene Hunchback in Drosophila. *Genetics* **138**, 125-134.
Ibanes, M. and Belmonte, J. C. (2008). Theoretical and experimental approaches to understand morphogen gradients. *Mol. Syst. Biol.* **4**, 176.
Kosman, D., Mizutani, C. M., Lemons, D., Cox, W. G., McGinnis, W. and Bier, E. (2004). Multiplex detection of RNA expression in Drosophila embryos. *Science* **305**, 846.
Lebrecht, D., Foehr, M., Smith, E., Lopes, F. J. P., Vanario-Alonso, C. E., Reinitz, J., Burz, D. S. and Hanes, S. D. (2005). Bicoid cooperative DNA binding is critical for embryonic patterning in Drosophila. *PNAS* **102**, 13176-13181.
Löhr, U., Chung, H.-R., Beller, M. and Jäckle, H. (2009). Antagonistic action of Bicoid and the repressor Capicua determines the spatial limits of Drosophila head gene expression domains. *Proc. Natl. Acad. Sci. USA* **106**, 21695-21700.
Lucchetta, E. M., Lee, J. H., Fu, L. A., Patel, N. H. and Ismagilov, R. F. (2005). Dynamics of Drosophila embryonic patterning network perturbed in space and time using microfluidics. *Nature* **434**, 1134-1138.
Lucchetta, E. M., Vincent, M. E. and Ismagilov, R. F. (2008). A precise bicoid gradient is nonessential during cycles 11-13 for precise patterning in the Drosophila blastoderm. *PLoS ONE* **3**, e3651.
Manu, Surkova, S., Spirov, A. V., Gursky, V. V., Janssens, H., Kim, A.-R., Radulescu, O., Vanario-Alonso, C. E., Sharp, D. H., Samsonova, M. et al. (2009). Canalization of gene expression in the *Drosophila Blastoderm* by gap gene cross regulation. *PLoS Biol.* **7**, e1000049.
Muramoto, T., Müller, I., Thomas, G., Melvin, A. and Chubb, J. R. (2010). Methylation of H3K4 is required for inheritance of active transcriptional states. *Curr. Biol.* **20**, 397-406.
Ochoa-Espinosa, A., Yu, D., Tsirigos, A., Struffi, P. and Small, S. (2009). Anterior-posterior positional information in the absence of a strong Bicoid gradient. *Proc. Natl. Acad. Sci.* **106**, 3823-3828.
Porcher, A. and Dostatni, N. (2010). The Bicoid morphogen system. *Curr. Biol.* **20**, R249-R254.
Pritchard, D. K. and Schubiger, G. (1996). Activation of transcription in Drosophila embryos is a gradual process mediated by the nucleocytoplasmic ratio. *Genes Dev.* **10**, 1131-1142.
Shermoen, A. W. and O'Farrell, P. H. (1991). Progression of the cell cycle through mitosis leads to abortion of nascent transcripts. *Cell* **67**, 303-310.
Sibon, O. C. M., Stevenson, V. A. and Theurkauf, W. E. (1997). DNA-replication checkpoint control at the Drosophila midblastula transition. *Nature* **388**, 93-97.
Simpson-Brose, M., Treisman, J. and Desplan, C. (1994). Synergy between the hunchback and bicoid morphogens is required for anterior patterning in Drosophila. *Cell* **78**, 855-865.
Sprague, B. L. and McNally, J. G. (2005). FRAP analysis of binding: proper and fitting. *Trends Cell Biol.* **15**, 84-91.
Wilkie, G. S., Shermoen, A. W., O'Farrell, P. H. and Davis, I. (1999). Transcribed genes are localized according to chromosomal position within polarized Drosophila embryonic nuclei. *Curr. Biol.* **9**, 1263-1266.
Xing, H., Vanderford, N. L. and Sarge, K. D. (2008). The TBP-PP2A mitotic complex bookmarks genes by preventing condensin action. *Nat. Cell Biol.* **10**, 1318-1323.